pH Responsive Decomposable Layer-by-Layer Nanofilms and Capsules on the Basis of Tannic Acid

Tatsiana Shutava, Malcolm Prouty, Dinesh Kommireddy, and Yuri Lvov*

Institute for Micromanufacturing and Chemistry Department, Louisiana Tech University, Ruston, Louisiana 71272

Received November 17, 2004; Revised Manuscript Received January 10, 2005

ABSTRACT: Tannic acid (TA) was assembled in alternation with two different polycations, strong poly(dimethyldiallylamide) (PDDA) and weak poly(allylamine) (PAH), using a layer-by-layer technique. Their deposition at different pH was confirmed by QCM, UV−vis spectroscopy, and surface charge measurements. TA/polyelectrolyte multilayer films and capsules have pH-dependent structural properties different from those of commonly used poly(styrenesulfonate)/poly(allylamine) (PSS/PAH) compositions. The lowest speed of TA/polycation multilayer dissolution was found at the conditions close to those used for film preparation. Permeability for fluorescein-labeled dextrans into tannic acid/polycation capsules with a five bilayer wall composition was investigated as a function of pH using confocal microscopy. It was found that minimal permeability occurs at pH 5−7 and maximal permeability at very high and very low pH, providing new opportunities for capsule loading as compared with an established procedure for PSS/PAH microcapsules. For TA/PDDA layers, less soluble films and less permeable capsules were obtained as compared with TA/PAH layers.

Introduction

The development of methods to form ultrathin organic films and microshells with tunable properties is of great interest. Layer-by-layer (LbL) electrostatic assembly was introduced as a method allowing construction of multilayers with nanometer precision and predetermined layer composition.[1] Among the species used for LbL assembly are polyelectrolytes, nanoparticles, DNA, and enzymes as well as lower molecular weight substances such as porphyrins.[1,2] The shells consisting of ordered polyelectrolyte layers can be formed over microcores, such as latex and inorganic microparticles, enzyme complexes, and drug crystals, providing modification of their solubility, biocompatibility, stability, and other properties.[2] It has been demonstrated that changing environmental pH or ionic strength of solutions can result in the formation of films with porous structure[3] or lead to partial decomposition of some assemblies.[4,5] Despite such properties which may provide control over release of drug encapsulated in polyelectrolyte capsules, the decomposable combinations of polyelectrolyte complexes are very limited.[3,4] Salt-induced deconstruction of layered DNA/polyelectrolyte assemblies was reported;[5a,b] however, it requires very high salt concentrations, which are not possible at physiological conditions. Application of poly(β-aminoesters) for hydrolytically decomposable films was also proposed.[5c] Therefore, a search for macromolecule materials suitable for degradable LbL membranes with tunable properties is of great interest.

Tannic acid (TA) belongs to the group of high molecular weight polyphenolic compounds, also known as hydrolyzable tannins, and contains a central carbohydrate (glucose) core, which is esterified by phenols (gallic acid) (Figure 1). Tannins originate from plants and microorganisms and are well-known because of their ability to precipitate proteins, such as collagen, gelatin, albumin, some polysaccharides, and alkaloids from solution.[6−8] Binding of the proteins by tannins is pH-dependent. The amount of precipitated protein depends on the conditions used, and no precipitation takes place at extremely low or high pH.[8] Moreover, protein precipitation by some tannins depends on temperature.[7c] Tannins interact with specific sites of proteins forming strong noncovalent bonds with such hydrophobic moieties of proteins as proline and histidine residues, but interaction with arginine, a positively charged site, was also reported.[6,8] Acidic properties of TA were seldom mentioned,[6−8] but no systematic investigation was reported and the ionization of galloyl phenol group is usually ignored. The only available pK_a value of TA is 2.5,[9a] and it appears to be unexpectedly low for phenols. Because of their ability to form intra- and intermolecular hydrogen bonds, polyphenols often exist in solution as loosely bounded complexes of several molecules, which can influence apparent behavior of the substances.[6−8] A few researches were reported on adsorption of phenols and polyphenols on polymers,[9] but none of them include amine-based polyelectrolytes or LbL-assembled films and capsules.

Taking into account properties of tannic acid,[6−9] we assume that tannins can be used as negatively charged structural blocks for LbL assembly in alternation with positive polyions. Two different polycations were chosen to be assembled: strong poly(dimethyldiallylamide) (PDDA) and weak poly(allylamine) (PAH).[1,2] As a primary amine, PAH can form hydrogen bonds with phenolic rings of TA through formation of hydrogen-centered complexes,[10−12] but formation of such bonds is not possible in the case of PDDA. Since tannic acid is a weak polyacid, strong influence of pH on properties of the multilayers based on TA is expected. Tannins and other derivatives of gallic acid have been recognized as substances with high biological activity, including antioxidant,[13] antimicrobial, and antiviral[14] properties, which allows future introduction of coatings with protective properties.

10.1021/ma047629x CCC: $30.25
Published on Web 03/02/2005

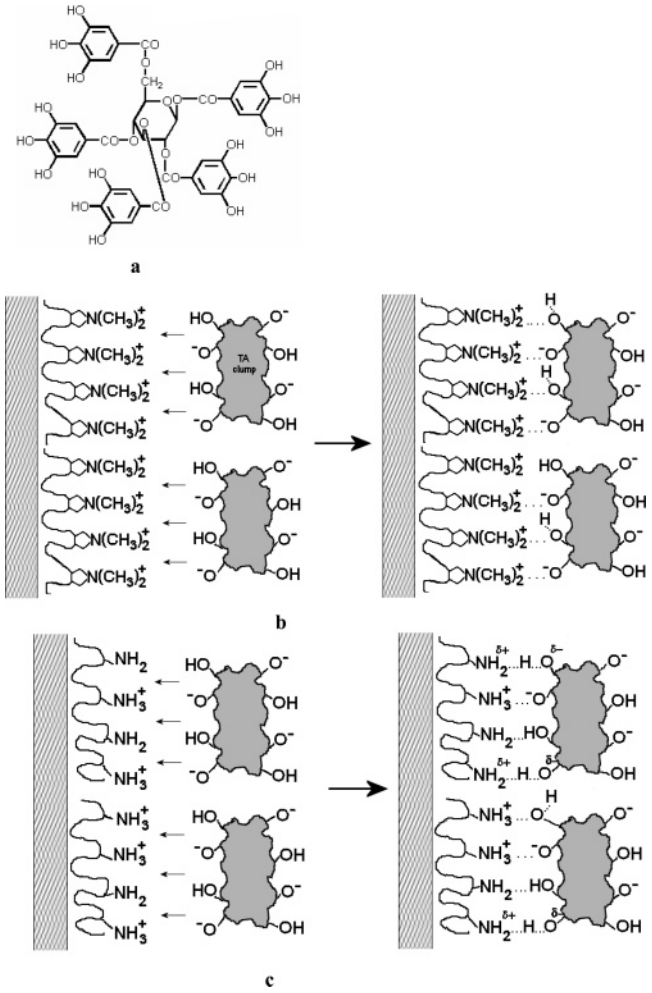

Figure 1. Chemical structure of tannic acid (a) and possible bond formation models of polyamine−tannic acid interaction in LbL films for PDDA (b) and PAH (c).

Experimental Section

Materials. Tannic acid (TA, 90% pentagalloyl glucose, MW 1701), sodium poly(styrenesulfonate) (PSS, MW 70 000), poly(dimethyl diallylamide) (PDDA, MW 100 000−200 000), poly(allylamine hydrochloride) (PAH, MW 70 000), sodium chloride, sodium carbonate, hydrochloric acid, sodium hydroxide, and Folin-Ciocalteu reagent were purchased from Sigma-Aldrich and used as received.

Film Deposition. $(PDDA/TA)_n$ and $(PAH/TA)_n$ ($n = 6-6.5$) films were deposited by sequential dipping of $1 \times 2 \times 0.1$ cm^3 glass slides into 3.0 mg/mL solutions of a polycation (PAH or PDDA) and TA at pH 4.0, 7.0, or 9.0 for 10 min per layer with two intermediate washings in DI water using an automated dipping machine. In a separate series of experiments, the films were also assembled on $0.9 \times 1.8 \times 0.09$ cm^3 quartz slides, and the deposition of each layer was followed by UV−vis spectroscopy (Agilent 8453 spectrometer).

The film thickness was estimated by the quartz crystal microbalance (QCM) technique. The films were deposited on QCM silver resonators in the same way as it was done for films on slides with the exception that the films were dried after deposition of each layer, and the resonator frequencies were measured. The frequency change (ΔF) of the resonators was monitored using a QCM instrument (USI-System, Japan) and converted into thickness or mass using the Sauerbrey equation Δd (nm) $= -0.016\Delta F$ (Hz), an empirical formula for 9 MHz electrodes, or Δm (ng) $= -0.84\Delta F$ (Hz). The detailed description of the procedure can be found elsewhere.[15] The value of bilayer thickness was calculated for TA/polycation films.

The amount of tannic acid in the films was estimated using the Folin-Ciocalteu assay for polyphenols.[16] A glass slide with a TA-containing film on it was immersed into 6 mL of DI water, and 1 mL of Folin-Ciocalteu reagent was added. The content was mixed and allowed to stand for 7−8 min at room temperature. Then 10 mL of a 7% sodium carbonate solution was added, followed by addition of water to 20 mL. The solution was mixed and allowed to stand for 2 h at room temperature. The concentration of TA was determined using absorbance at 765 nm. TA in solution was used for calibration. Beforehand, it was shown that the interference of PAH and PDDA with the assay is negligible.

Film Dissolution Procedure. The $(PDDA/TA)_6$/PDDA or $(PAH/TA)_6$/PAH films deposited on glass slides were immersed into 3 mL of DI water with a pH value in the range of 1.0−10.0 in a quartz cuvette. With 0.5−10 min intervals, the slides were removed, and UV−vis spectra of the solutions were recorded. The TA concentration in the solutions was estimated from absorbance at 280 nm (the wavelength corresponds to the neutral form of TA) using extinction coefficients experimentally obtained for TA solutions at a given pH.

Shell Assembly on Microcores and Preparation of Hollow Capsules. For capsule preparation, 0.5 mL (1.0 mL for the first TA layer) of a 3 mg/mL TA solution and a 2 mg/mL PAH or PDDA solution at pH 7.0 were added alternatively to 15 mL of a suspension containing 25 mg of $MnCO_3$ cores (diameter 7.0 μm, prepared according to ref 17). After 15 min adsorption of each layer, the particles were washed with DI water three times. In some cases, two PSS/PAH bilayer precursor films were additionally fabricated on carbonate cores by alternative adsorption of anionic PSS and cationic PAH from 3 mg/mL solutions in 0.5 M NaCl at pH 7.0.[2] The assembly was monitored with surface potential (ξ-potential) measurements using a Brookhaven Zeta Plus microelectrophoretic instrument. For dissolution of $MnCO_3$ cores, the obtained particles were resuspended in 2 mL of a 0.1 M EDTA solution at pH 7.0. After 4 h at room temperature the supernatant was replaced with a new portion of EDTA solution for 12 h. Finally, the capsules were rinsed with DI water three times. $(PSS/PAH)_2/(TA/PAH)_3$ capsules were prepared in the same way as above. Atomic force microscopy (AFM) images of dried capsules on mica were taken using a Q-Scope 250 Quesant instrument in intermittent-contact mode. Confocal laser scanning microscopy (Leica DMI RE2) was used to analyze the structure of the obtained microcapsules.

Capsule Permeability Test. Fluorescein isothiocyanate (FITC, Sigma) and FITC-labeled dextrans (1 mg/mL, Sigma) with molecular weights of 4400, 77 000, and 2 000 000 were used for permeability test experiments. Typically, 20 μL of a capsule solution with pH adjusted with NaOH and HCl to the value under investigation were mixed with 20 μL of a dextran solution on a glass slide placed in the holder of the confocal microscope. One of the capsules was chosen, zoomed on, and the intensities of the light emitted by capsule interior (I_{int}) and by surrounding solution (I_{ext}) were measured 10 min after the mixing. The measurements were done for 7−11 capsules at each pH and averaged.

Results and Discussion

Layer-by-Layer Assembly on QCM Resonators. Tannic acid was assembled at different pH in alternation with strong (PDDA) or weak (PAH) polycations. The QCM data for TA in alternation with PDDA at different conditions are presented in Figure 2a. The film shows a stable tendency to grow with deposition of each layer. The thickness of PDDA/TA bilayers is ca. 3.8−5.8 nm and depends on the pH used for film assembly (Figure 2a, inset). For PDDA/TA compositions, thicker films were obtained at pH 4.0, where, as we assume, the negative charge density of TA macromolecules is smaller. Following the general tendency of electrostatic assembly of polyelectrolytes,[1−3] TA/PDDA film thickness decreases with increasing charge density at higher pH.

For TA/PAH combinations, the assembly features are slightly different (Figure 2b). An excess deposition of

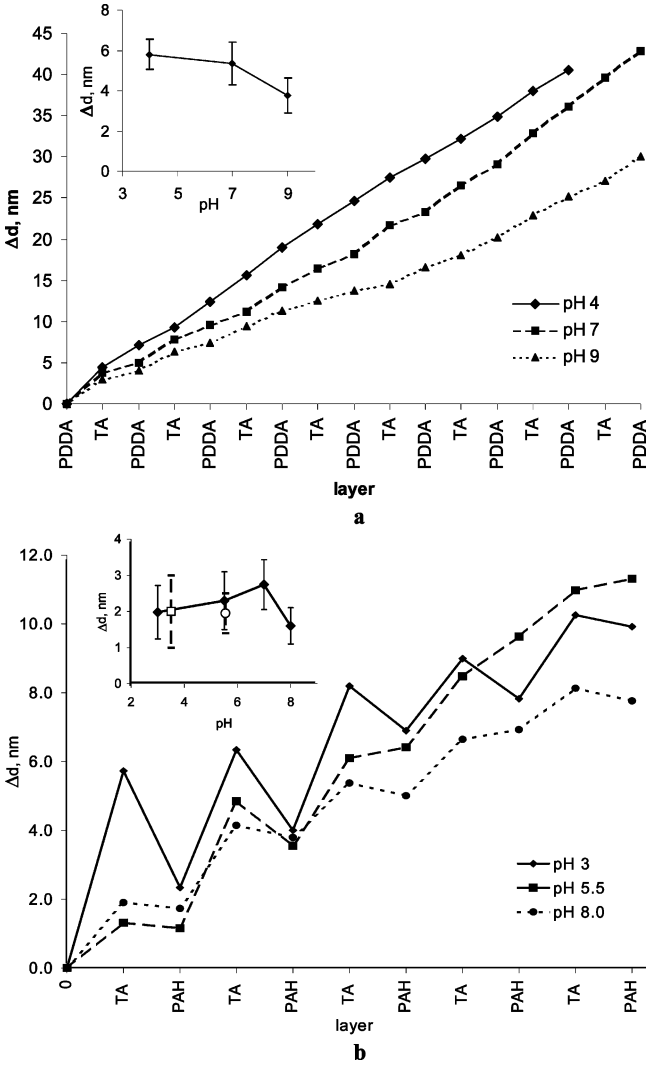

Figure 2. QCM results for deposition of TA in alternation with PDDA (a) and PAH (b). The insets show dependence of tannic acid/polycation bilayer thickness on pH; open symbols correspond to assemblies prepared at pH 4.0 for TA layers and pH 3.5 (□) and 5.5 (○) for PAH layers.

TA on PAH layers was observed. The film thickness increases by 1.2−5.7 nm for a single TA layer and then decreases after deposition of the next PAH layer; the phenomenon is higher at low pH and more noticeable for the first 2−3 bilayers. Such an "up/down" mode was often observed for alternation of polymers and multicharged connectors, such as sulfonated porphyrines, and explained by dye aggregation.[1e] Besides, the thickness of a TA layer deposited on the top of a PAH layer decreases with increasing number of TA/PAH layers in the films. At pH 3.0, the estimated thickness drops from 5.7 nm for the first TA layer to ∼2.2 nm for the 4−5th layer. At pH 5.5 and 8.0, the corresponding changes are smaller (from ∼2.2 to 1.2 nm). The reason for such tendency remains unclear and may be related to aggregation and nonuniformity of bulk films. However, the higher thickness of TA layers at pH 3.0 can be explained by increased hydrophobic aggregation of TA molecules uncharged at low pH. For both TA/PDDA and TA/PAH assemblies, the thickness of initially deposited polyphenol layers is much higher than any dimension of a single TA molecule ($1.85 \times 1.65 \times 1.01$ nm^3).[8c] The ability of polyphenols to form self-aggregates in solution is a well-known phenomenon,[7,8] and we assume that such aggregates, not single TA molecules, were deposited.

Table 1. Amount of Tannic Acid in Films (Folin-Ciocalteu Assay)

polyelectrolytes	pH of assembly	m_{TA}(F−C) × 10^6, g/cm^2	m_{film}(QCM) × 10^6, g/cm^2	% TA in film
TA/PDDA	4.0	0.82	1.83	45
	7.0	0.90	1.53	59
	9.0	0.60	1.06	57
TA/PAH	7.0	0.73 ± 0.12	1.07	68

The average thickness of TA/PAH bilayers was found to vary from 1.6 to 2.7 nm, being maximal for the films assembled at pH 7 (Figure 2b, inset). These conditions seem to be the best for obtaining stable, thick TA/PAH films. Slight differences of pH for tannic acid and polycation solutions do not influence the bilayer thickness.

The step growth of films on QCM resonators (Figure 2a) shows that TA introduces about 50% of total thickness (and mass) in TA/PDDA films. These data are in good agreement with the results of the Folin-Ciocalteu assay for $(TA/PDDA)_6$/PDDA films (Table 1). A slightly higher amount of the polyphenol was found in TA/PAH multilayers compared with that in TA/PDDA layers. It can be related with the excess deposition of tannic acid on PAH layers.

UV−Vis Spectra of Tannic Acid in Solution. In aqueous acidic solution the absorption spectrum of tannic acid exhibits two peaks at 214 and 271 nm (Figure 3a) assigned to its neutral form and consistent with the spectra in the UV range previously reported for TA.[18] At higher pH values, absorbance for both peaks is smaller, and both peaks slightly shift their positions to higher wavelengths. Besides, a shoulder at 233 nm and a peak at 315 nm appear, and their intensities increase with increasing pH. The presence of two isosbestic points at 223 and 284 nm (289 nm in the case of increasing pH) supports the assumption that at least two different forms of tannic acid, convertible from one into another, may be present in the solution. Taking into account the available data on optical properties of phenols,[18c,d,19a] we assume that the peaks at 233 and 315 nm belong to the phenolate form of tannic acid. Slightly different peak positions were observed in the case when the spectra recording was started in basic solutions and pH was adjusted to lower values by sequential addition of a 0.1 M HCl solution (Supporting Information, Figure A). The observed shift may be due to variable self-association of the polyphenol at different pH.[6−8]

Figure 4a shows how the ratio of the absorbance at 315 and 271 nm (the ratio of the ionized and neutral forms of TA) depends on pH. From the equivalence point on the curves,[19] we estimated the apparent dissociation constant (pK_{app}) values of TA to be 3.2 and 2.2 for increasing and decreasing pH, respectively. The obtained pK_{app} values are comparable with the only available value (ca. 2.5) estimated from surface charge measurements of iron oxide colloids precipitated by TA.[20] These values also correlate with our data on pH dependence of surface charge for TA-coated microparticles (see data on TA deposition on cores below). No systematic data are available on ionization behavior of tannic acid. We obtained pK_{app} values somewhat higher than usually expected for phenols (pK_a 9.9), even for those that have electron-withdrawing substitutive groups in the ring.[10b,c] Recently, the critical ionization model

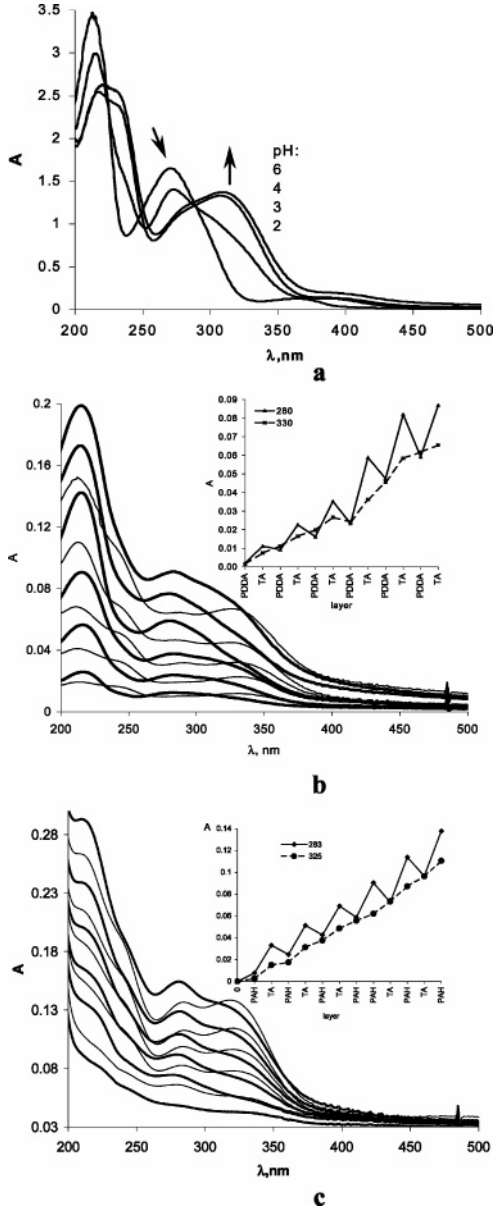

Figure 3. UV−vis spectra: (a) a 0.0375 mg/mL TA solution at different pH; (b) a TA/PDDA film after deposition of a PDDA (fine line) and TA (solid line) layer, pH 7.0; (c) a TA/PAH film after deposition of a PAH (fine) and TA (solid) layer, pH 7.0. The insets in (b) and (c) show the step growth of absorbance at wavelengths corresponding to phenolate and neutral forms of TA as a function of deposited layer.

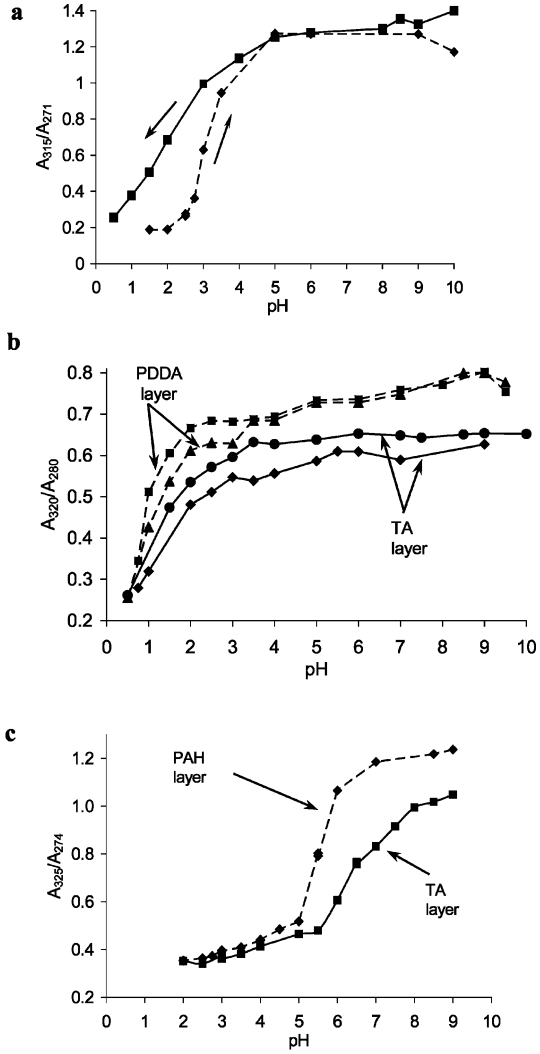

Figure 4. Ratio of phenolate to neutral form absorbance for tannic acid at different pH: (a) 0.0375 mg/mL TA solution; (b) $(PDDA/TA)_6$ and $(PDDA/TA)_6$/PDDA films; (c) $(PAH/TA)_6$ and $(PAH/TA)_6$/PAH.

was proposed to explain "hyperacidic" hydroxyl groups of some synthetic polyphenols.[21] The ability of polyphenols to form intramolecular hydrogen bonds stabilizes monoanions by distributing the anionic charge efficiently over several atoms. This effect grows as the number of phenolic units participating in the distribution of charge increases. Moreover, the participating hydroxyl groups can be separated much further in space, and all acidic sites can be treated as energetically equal. Each molecule of tannic acid (pentagalloylglucose) has 15 hydroxyl groups attached to 5 phenol rings, and therefore, its pK_{app} may be much lower than that for monophenols.[21] Besides, one should take into account that the obtained values characterize only pK_{app} of the phenolic groups responsible for spectral changes, and spectral properties of tannins may vary from source to source.[18]

UV−Vis Spectra of TA/PDDA Multilayers. Figure 3b shows UV−vis spectra of a PDDA/TA film in the process of LbL assembly. Since PDDA in solution has only slight absorbance in the far-UV region, we assume that the spectrum of TA/PDDA films mostly corresponds to that of TA. While tannic acid is assembled with PDDA (pH 7.0), its spectrum shifts to higher wavelengths compared with that in solution. The shift of the peak positions can be caused by different charge distribution in TA molecules as a result of conjugation with amide moiety in PDDA. In analogy with the behavior of TA in solution, we assume that the peaks at 215 and 280 nm correspond to the neutral form of TA, while the peaks at 247 and 330 nm correspond to the ionized TA molecules. The relative contributions of these peaks depend on the nature of the outermost layer. When TA is the upper layer, two peaks at 215 and 280 nm are observed with slight shoulders at the positions corresponding to the ionized form. Deposition of the following PDDA layer causes a decrease of intensity for these two peaks and an increse for the peaks at 247 and 330 nm. One can see that the deposition of PDDA results in additional ionization of TA molecules (Figure 3b, inset). Similar ionization oscillation was previously found for

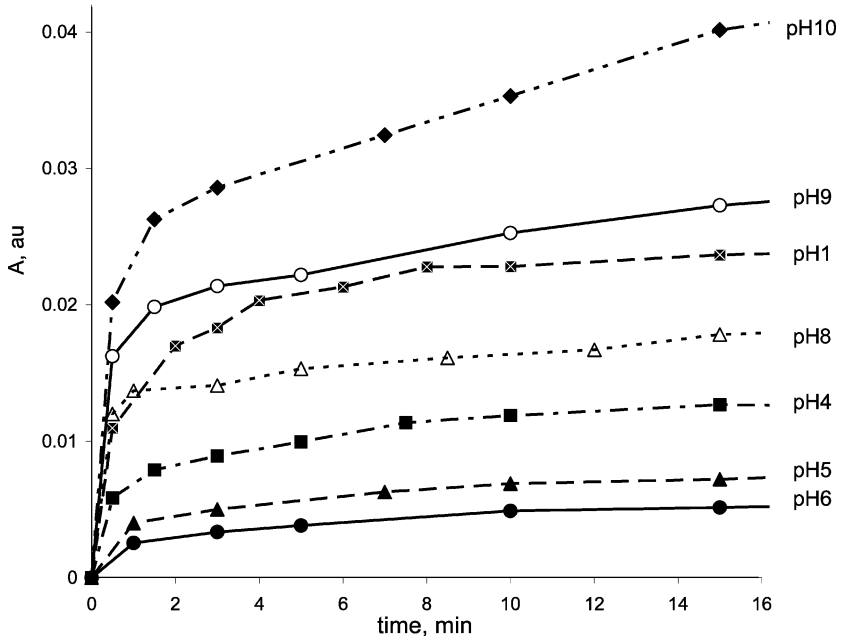

Figure 5. Dissolution kinetics of $(PDDA/TA)_6$/PDDA films prepared at pH 7.0 in water at different pH.

several other assemblies and explained by additional protonation−deprotonation of the components as a result of charge adjustment within a few layers from the film surface.[1e,22]

The phenolate/neutral form absorbance ratios for TA/PDDA films at different pH are shown in Figure 4b. From the equivalence points on the curves, we estimated pK_{app} values of TA to be smaller than 0.75 and 1.0 for films with PDDA and TA as the outermost layers, respectively. This means that the 1.5−2.5 unit shift of pK_{app} for tannic acid is observed due to assembly with such strong polycations as PDDA. Additionally, at pH less than 1, the shift of TA peaks in film spectra decreases, reaching the value for free uncharged TA in solution (Figure A in Supporting Information). Our observation corresponds to the results of several research groups on increased ionization of polyanions participating in LbL assembly.[3,23]

UV−Vis Spectra of TA/PAH Multilayers. Changing PDDA for PAH does not significantly influence the peak positions in the film spectra (Figure 3c). The spectrum of TA assembled with PAH moved to higher wavelengths compared to that in solution. The shift is 8 and 10 nm for neutral and phenolate forms against 5 and 15 nm for assemblies with PDDA. One can see (Figure 3c, inset) that absorbance of ionized and neutral forms of tannic acid in the TA/PAH films oscillates as a function of the outermost layer. However, the neutral form absorbance increases approximately on the same value for each layer of tannic acid. Previously for TA/PAH films on QCM resonators, an excess deposition of tannic acid was observed. It can result in slightly different absorbance changes with deposited layers for the films as compared with TA/PDDA films.

For TA/PAH films, the phenolate/neutral form absorbance ratio is shifted to higher pH values (Figure 4c). Estimated on the basis of the data, pK_{app} values (ca. 5.5 and 6.3 for films with PAH and TA layers, accordingly) are sufficiently higher than that for TA in solution and in the assembly with PDDA. The result is surprising because for weak polyelectrolytes in LbL films pK_{app} values obviously shift approximately 2−3 units toward the alkaline region for polycations or the acidic region for polyanions.[23] However, hydrogen bonding could influence the interaction. In such a case, significantly less ionization of charged specimens in assembled layers was observed.[4]

Tannic Acid−Polycation Interaction in TA/PDDA and TA/PAH Multilayers. One can find many references on phenol−amine conjugation in aqueous and organic solvents.[10−12] Hydrogen bonding in the systems was confirmed by different methods, such as NMR and IR spectroscopy,[10a−f] viscosimetry,[10g] and precipitation of phenol−amine crystals[10e] as well as indirectly by influence of amines on phenol oxidation.[11] Several mathematical models[12] have been proposed to optimize structures of such complexes. However, the investigation of hydrogen bonding in the complexes is complicated by numerous factors that contribute to their structure, such as interactions between different parts of the molecules in the complexes, possibility of solvent participation, etc.

In accordance with previously reported data on interactions between phenol derivatives and amines,[10−12] we propose that the difference in polyphenol/polyamine bonding significantly influence properties of formed complexes for various amine-based polyelectrolytes. At pH 7, clumps of tannic acid apparently have charged and uncharged groups on the surface. We assume that at interaction of TA and PDDA, which is completely charged at pH 7.0, new polar bonds form between charged sites as well as additional ionization of uncharged sites of tannic acid occurs (Figure 1b). In the case of PAH the picture is different. At pH 7, PAH (pK_a of PAH ca. 8.7 in solution and 10.7 in PSS/PAH films[23a]) is partially uncharged. Forming bonds probably include electrostatic interaction between charged sites of tannic acid and PAH as well as several different types of conjugation between $-NH_2$ ($-NH_3^+$) and $-OH$ ($-O^-$) groups, resulting in formation of hydrogen-centered bonds (Figure 1c).

Dissolution Kinetics for TA/PDDA Multilayers. Figure 5 shows dissolution kinetics of $(PDDA/TA)_6$/PDDA films at different pH. Initial dissolution is very fast but slows down with time. The lowest dissolution speed was found at the conditions that are close to those

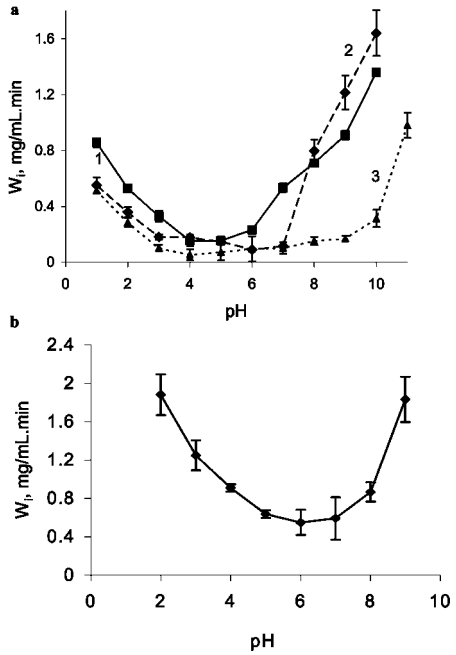

Figure 6. Initial rate of film dissolution (W_i) vs pH: (a) $(TA/PDDA)_6$ films prepared at pH 4 (1), pH 7 (2), and pH 9 (3); (b) $(TA/PAH)_6$ films prepared at pH 7.0.

used for film preparation (Figure 6a). It is quite understandable considering charge compensation within the films. The observed very light dissolution under these conditions can be a result of extraction of TA molecules from the films into surrounding solution (water). The films are constructed from clumps of TA linked to the polycation, but some TA molecules inside the clumps are coupled loosely and can be released. For TA/PDDA films, the rate of dissolution remains low over the pH region between pH of film preparation (4, 7, or 9 accordingly) and pH 4. It accelerates at pH below 4 apart from the pH used for film preparation. At these low pH values, TA molecules are less charged and the films become unstable. However, dissolution behavior of the TA/PDDA films in basic solutions is surprising assuming that both TA and PDDA should be completely charged at these conditions. In basic solutions above pH of preparation, film dissolution is very fast (Figure 6a). An additional increase in charge density of anionic TA layers overcomes the attraction of TA and PDDA in the layers. Further shift of TA peak positions to higher wavelengths (Figure A in Supporting Information) can be considered as an indirect evidence of increasing charge of TA. Besides, solubility of phenolic compounds is higher at basic pH, and the dissolution can be affected by extraction of TA molecules from the films.

Dissolution Kinetics for TA/PAH Multilayers. Dissolution patterns similar to TA/PDDA films were found for $(PAH/TA)_6/PAH$ films (Figure 6b). The films dissolve with increased rate in acidic and basic solutions. The lowest rates of dissolution were also observed at pH 6−7; the conditions are close to that of film preparation. At pH lower than 6.0, the amount of the phenolate form of TA in the films rapidly decreases (Figure 4c). In contrast, above pH 8, PAH becomes less charged (pK_a of PAH ca. 8.7 in solution and 10.7 in PSS/PAH films[23a]). Changes of charge densities loosen the films. One can see that the rate of TA/PAH film dissolution is 3−6 times higher than that of TA/PDDA films at the same conditions (Figure 6), indicating a less bound structure of TA/PAH films.

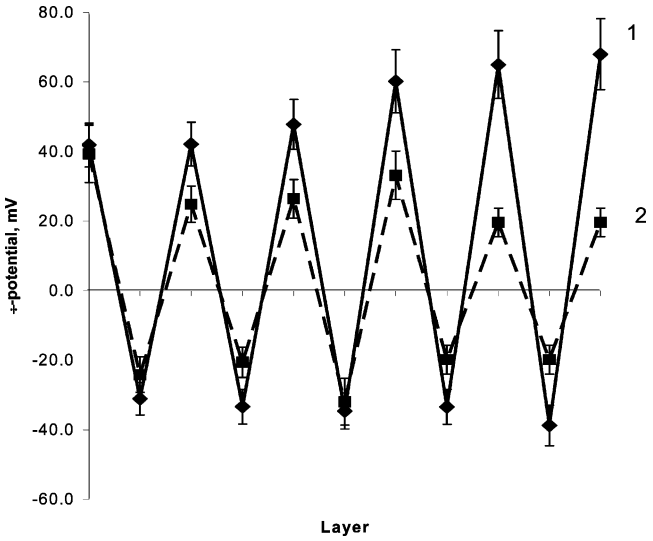

Figure 7. ξ-potential of microparticles as a function of deposited layer: 1, TA/PDDA; 2, TA/PAH; pH 7.0.

Polyelectrolyte Multilayer Shells on Microcores. The TA/PDDA and TA/PAH shells were deposited on $MnCO_3$ microcores at pH 7.0. Figure 7 shows the alternating changes of surface charge of the particles after deposition of each layer. Initially, positively charged cores became negatively charged after deposition of a TA layer. Deposition of the next PDDA or PAH layer shifts the surface charge of the particles again to a positive value, in agreement with LbL assembly principles.[1] An attempt was made to determine the isoelectric point of the microparticles with TA as the outermost layer (for $MF/(TA/PAH)_2/TA$ microshells): it was found that down to pH 4.0 the particles are slightly negative with a surface charge of -14.0 ± 5.0 mV. At pH 3.5, the particles were strongly positive (50.3 ± 9.0 mV). Unfortunately, since at low pH fast dissolution of the films containing TA takes place, one cannot say whether the last highly positive value still characterizes the assembly.

Microcapsules on the Basis of Tannic Acid. $(TA/PDDA)_5$ and $(TA/PAH)_5$ empty capsules were prepared as described in the Experimental Section. Figure 8a shows confocal images of the TA/PDDA capsules with a diameter of 7.0 μm after dissolution of inner $MnCO_3$ cores. Capsule walls are smooth without noticeable defects. Many of the TA/PAH capsules have defects in the walls (Figure 8b, indicated by arrow) that do not influence the capsule integrity and may result from partial collapse of the walls. When the two inner TA/PAH layers in the capsules are replaced by two PSS/PAH layers, the capsules obtained after core dissolution have very uneven, ragged wall structure with numerous gaps and bulges (Figure 8c). The unusual structure can appear as a result of the damaging influence of TA on previously absorbed polyelectrolyte layers or, on the other hand, originate from thick wall corruption during core dissolution in relatively aggressive medium.

Figure 9a shows an AFM image of a dried five bilayer $(TA/PAH)_5$ capsule. The roughness of the capsule surface is much higher than that usually observed for PSS/PAH multilayered capsules (Figure 9b). Aggregates ranging in size from 200 to 300 nm are observed on the surface of $(TA/PAH)_5$ capsules. Some smaller structures with a diameter less than 100 nm also can be seen in the image. The clusters seem to be tight complexes of

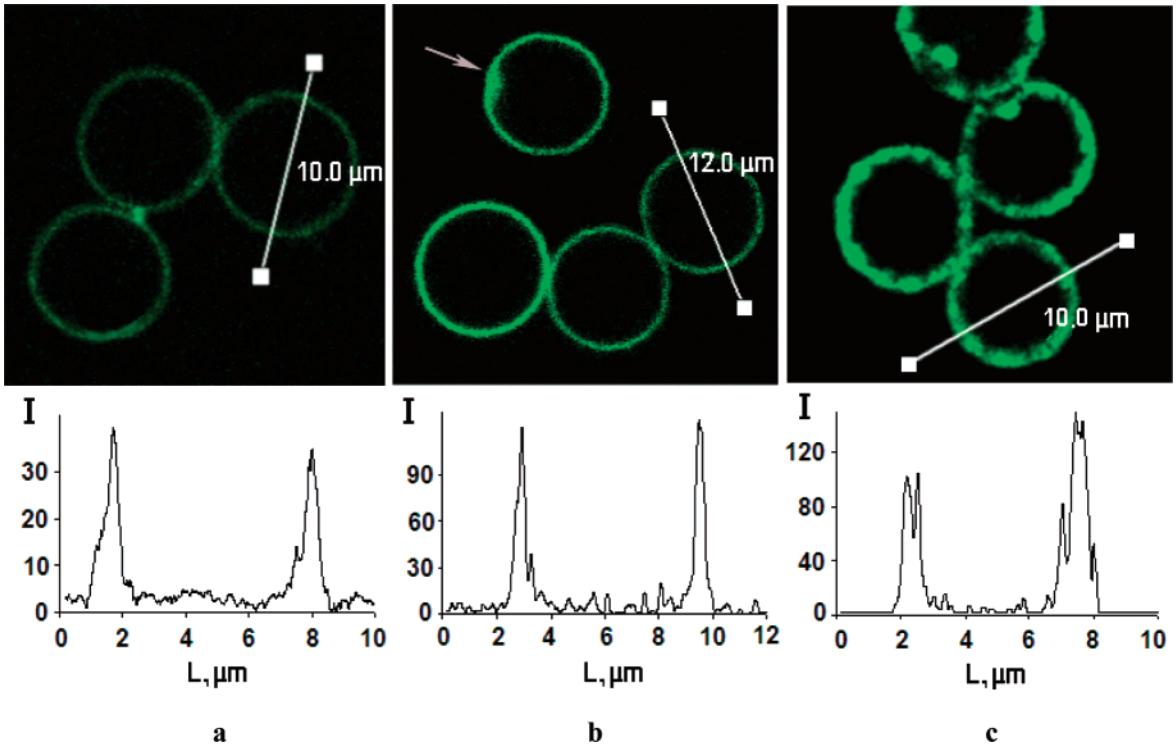

Figure 8. Confocal images of $(TA/PDDA)_5$ (a), $(TA/PAH)_5$ (b), and $(PSS/PAH)_2/(TA/PAH)_3$ (c) capsules in solution (capsules were stained with FITC) with corresponding profiles. The arrow indicates a capsule defect.

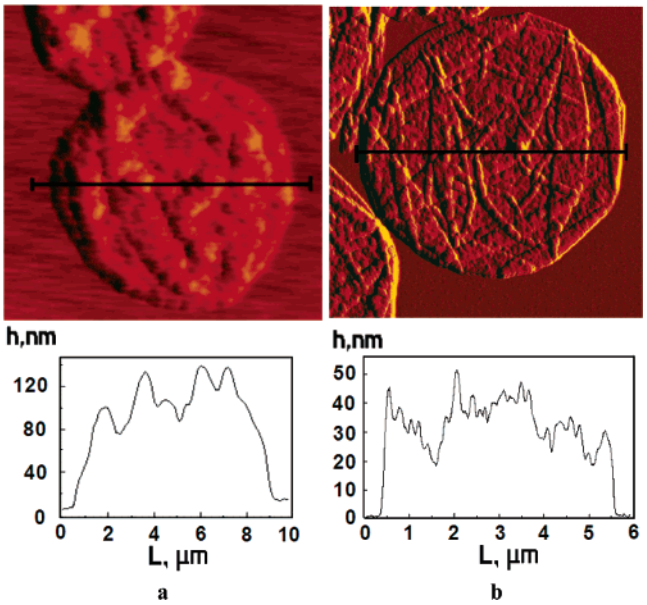

Figure 9. AFM images of a dried $(TA/PAH)_5$ (a) and $(PSS/PAH)_4$ (b) capsule with corresponding profiles.

TA and PAH. AFM imaging of polyphenolic acid clumps on mica surface was also recently reported.[20] Considering the shape and size of dried TA/PAH capsules and taking the density of solid residue as 1.1 g/cm^3, the mass of a hollow capsule can be estimated as $(4.1 \pm 0.4) \times 10^{-12}$ g. In another approach, taking the thickness of dried five bilayer capsule walls to be 20 ± 2 nm (QCM) and its diameter to be 7.0 ± 0.5 μm (confocal microscopy), one can calculate the mass of hollow capsule wall to be $(3.4 \pm 0.6) \times 10^{-12}$ g, which is in good agreement with the experimental data.

From minimal heights on AFM profiles for four $(TA/PAH)_5$ capsules we estimated the thickness of a tannic acid/PAH bilayer to be 5.7 ± 0.6 nm. The value is somewhat higher than that obtained by QCM (2.7 ± 0.7 nm at pH 7.0) with drying the films after deposition of each layer. Slightly different preparation conditions can influence the observed layer thickness.

Permeability of TA-Based Capsules. The images of $(TA/PDDA)_5$ and $(TA/PAH)_5$ capsules in solutions of FITC-dextrans at different pH are shown in Figure 10. The ratio of intensities emitted by capsule interiors and surrounding solution, 10 min after mixing the capsule suspension and dextran solutions, was used for evaluation of capsule wall permeability. For $(TA/PDDA)_5$ capsules, I_{int}/I_{ext} values lower than 1 were observed for polymer chains with MW 2 000 000 at all pH. The interior of capsules remains black for at least 30 min, indicating that labeled dextran chains cannot penetrate inside the capsules. The lowest permeability of the capsules was found at pH 6−7. Downward and upward, the ratio of interior/exterior intensities slightly increases, indicating that the fluorescent polymer slowly penetrates inside. For FITC-labeled dextran with MW of 77 000 and 4400, the permeability increases in good agreement with larger diffusion coefficient of substances with lower molecular weight. The minimum I_{int}/I_{ext} values were found over the pH 5−7 region. Finally, the capsules were permeable at any pH for low molecular weight FITC.

Permeability of $(TA/PAH)_5$ capsules for FITC-Dextran with MW 2 000 000 remains low only over the pH region of 5−7 (Figure 10b). Over the same region, the capsules are partially permeable for dextran of MW 77 000. No delayed interior fluorescence was found for substances of lower molecular weight.

Comparison of Permeability for Different Capsules. From the above data, one can conclude that both $(TA/PDDA)_5$ and $(TA/PAH)_5$ capsules have the lowest permeability at relatively mild conditions close to pH of capsule preparation. For both capsule types, perme-

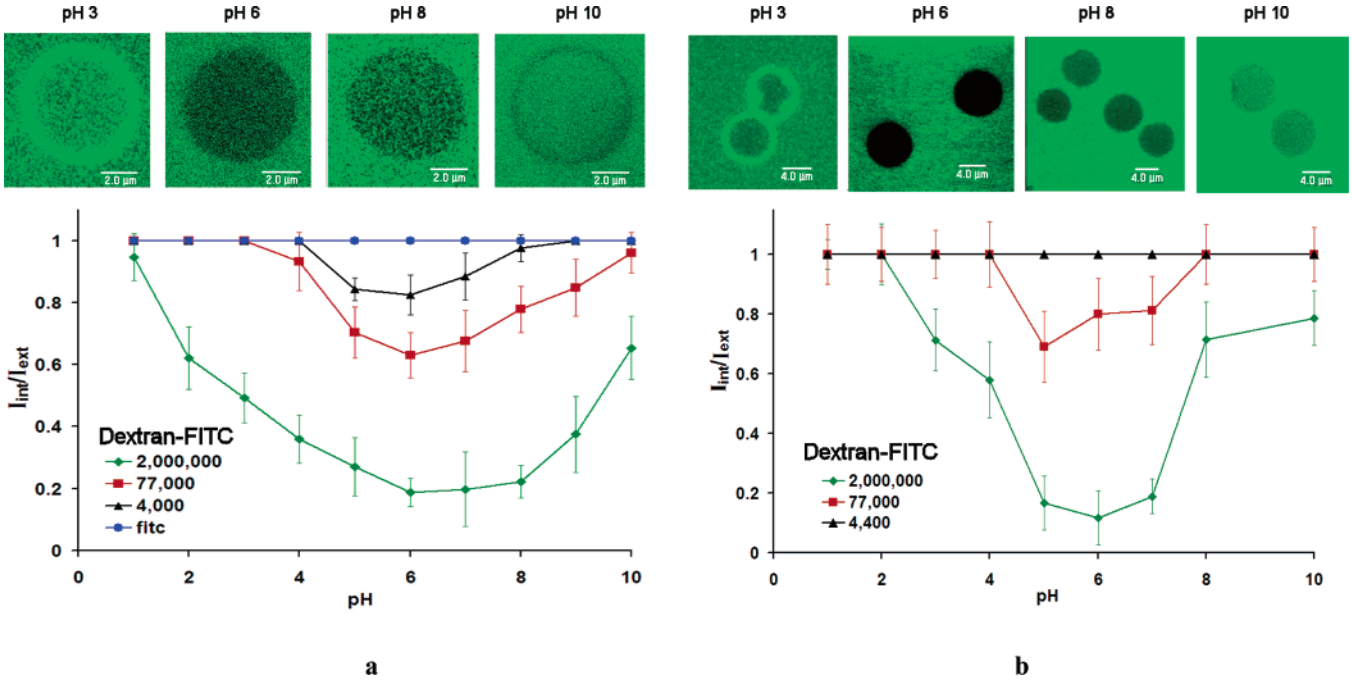

Figure 10. Ratio of intensities emitted by capsule interiors (I_{int}) and surrounding solution (I_{ext}) 10 min after mixing capsules and solutions of FITC-dextran of different molecular weights. (a) $(TA/PDDA)_5$ capsules; the upper row shows confocal images of the capsules in dextran-77000 at different pH. (b) $(TA/PAH)_5$ capsules; the upper row shows confocal images of the capsules in dextran-2000000 at different pH.

bility significantly increases both in low and in high pH regions. One can see that permeability of capsules based on tannic acid is different from commonly used PSS/PAH capsules.[24] PSS/PAH capsules usually are considered sealed for high molecular weight substances at pH above 7.0 and open at pH lower than 7.0. At the same time, the PSS/PAH capsules are completely permeable at all pH for substances with molecular weight lower than several thousands. Unlike PSS/PAH capsules, TA/PDDA capsules show delayed interior fluorescence in the case of dextran with MW 4000. Also, TA/PAH capsules seem to be even more permeable for dextran with MW 77 000 than PSS/PAH capsules.

The permeability features of the capsules containing TA highly correlate with the dissolution kinetics observed for corresponding films at different pH. For TA/PDDA, less soluble films and less permeable capsules were obtained as compared with TA/PAH layers. The phenomenon apparently can be explained by formation of a more bound structure in the case of TA/PDDA assemblies compared with those for TA/PAH.

Conclusion

An introduction of polyphenols into layer-by-layer self-assembly expands the range of components, which can be incorporated into the films. Tannic acid can be LbL-assembled with weak and strong positive polyelectrolytes into the multilayers, the stability of which varies with environmental conditions. Capsules and films designed with tannic acid show pH-dependent permeability with strong minimum between pH 5 and 7, which is different from that of commonly used PSS/PAH microcapsules. It extends possible applications of multilayered polyelectrolyte membranes in controlled drug release systems. In particular, the polyelectrolyte microcapsule loading−release profile may be better adjusted. Alternation of tannic acid with positively charged natural polyelectrolytes with primary amine groups (e.g., chitosan) or proteins allows new biodegradable assemblies. Additionally, an application of polyphenols for LbL assembly may help to introduce antioxidant activity for films and capsule shells, providing by this active defense system.

Acknowledgment. This work is partially supported by NSF #0210298 and NIH-1RO1 EB00739-01 grants. Any opinions, findings, conclusions, or recommendations expressed in this material are those of the authors and do not necessarily reflect the view of the National Science Foundation or National Institute of Health. We are thankful to Dr. S. Sukhishvili for useful critic and discussion.

Supporting Information Available: Figure showing shift of absorbance maxima of the neutral form of TA at different pH. This material is available free of charge via the Internet at http://pubs.acs.org.

References and Notes

(1) (a) Decher, G. *Science* **1997**, *227*, 1232. (b) Lvov, Y.; Ariga, K.; Ichinose, I.; Kunitake, T. *J. Am. Chem. Soc.* **1995**, *117*, 6117. (c) Shiratori, S. S.; Rubner M. F. *Macromolecules* **2000**, *33*, 4213. (d) Lvov, Y.; Lu, Z.; Schenkman, J.; Rusling, J. *J. Am. Chem. Soc.* **1998**, *120*, 4073. (e) Agira, K.; Lvov, Y.; Kunitake, T. *J. Am. Chem. Soc.* **1997**, *119*, 2224. (f) Schlenoff, J. B.; Ly, H.; Li, M. *J. Am. Chem. Soc.* **1998**, *120*, 7626.

(2) (a) Sukhorukov, G. Multilayer Hollow Microspheres. In *Dendrimers*; MML Series; Citus Books: New York, 2002; Vol. 5, p 111. (b) Lvov, Y.; Antipov, A.; Mamedov, A.; Möhwald, H.; Sukhorukov, G. *Nano Lett.* **2001**, *1*, 125. (c) Ai, H.; Jones, S.; deVilliers, M.; Lvov, Y. *J. Controlled Release* **2003**, *86*, 59. (d) Gao, C.; Liu, X.; Shen, J.; Möhwald, H. *Chem. Commun.* **2002**, 1928. (e) Antipov, A.; Shchukin, D.; Fedutik, Y.; Zanaveskina, I.; Klechkovskaya, V.; Sukhorukov, G.; Möhwald, H. *Macromol. Rapid Commun.* **2003**, *24*, 274. (f) Sukhorukov, G. B.; Antipov, A. A.; Voigt, A.; Donath, E.; Möhwald, H. *Macromol. Rapid Commun.* **2001**, *22*, 44.

(3) (a) Mendelsohn, J. D.; Barrett, C. J.; Chan, V. V.; Pal, A. J.; Mayes, A. M.; Rubner, M. F. *Langmuir* **2000**, *16*, 5017. (b) Yoo, D.; Shiratori, S. S.; Rubner, M. F. *Macromolecules* **1998**,

31, 4309. (c) Zhai, L.; Nolte, A. J.; Cohen, R. E.; Rubner, M. F. *Macromolecules* **2004**, *37*, 6113.
(4) Sukhishvili, S. A.; Granik, S. *Macromolecules* **2002**, *35*, 301. Kozlovskaya, V.; Ok, S.; Sousa, A.; Libera, M.; Sukhishvili, S. *Macromolecules* **2003**, *36*, 8590.
(5) (a) Dubas, S. T.; Schlenoff, J. B. *Macromolecules* **2001**, *34*, 3736. (b) Schuler, C.; Caruso, F. *Biomacromolecules* **2001**, *2*, 921. (c) Vazquez, E.; Dewitt, D. M.; Hammond, P. T.; Lynn, D. M. *J. Am. Chem. Soc.* **2002**, *124*, 13992.
(6) Haslam, E. *J. Nat. Prod.* **1996**, *59*, 205.
(7) (a) Van Buren, J. P.; Robinson, W. B. *J. Agric. Food Chem.* **1969**, *17*, 772. (b) Osawa, R.; Walsh, T. P. *J. Agric. Food Chem.* **1993**, *41*, 704. (c) Hegerman, A. E.; Rice, M. E.; Ritchard, N. T. *J. Agric. Food Chem.* **1998**, *46*, 2590. (d) Edelmann, A.; Lendl, B. *J. Am. Chem. Soc.* **2002**, *124*, 14741. (e) Frazier, R. A.; Papadopoulou, A.; Mueller-Harvey, I.; Kissoon, D.; Green, R. J. *J. Agric. Food. Chem.* **2003**, *51*, 5189.
(8) (a) Baxter, N. J.; Lilley, T. H.; Haslam, E.; Williamson, M. P. *Biochemistry* **1997**, *36*, 5566. (b) Charlton, A. J.; Baxter, N. J.; Khan, M. L.; Moir, A. J. G.; Haslam, E.; Davies, A. P.; Williamson, M. P. *J. Agric. Food. Chem.* **2002**, *50*, 1593. (c) Madhan, B.; Dhathathreyan, A.; Subramanian, V.; Ramasami, T. *Proc. Indian Acad. Sci. (Chem. Sci.)* **2003**, *115*, 751.
(9) (a) Chibowski, E.; Espinosa-Jimenez, M.; Ontiveros-Ortega, A.; Gimenez-Martin, E. *Langmuir* **1998**, *14*, 5237. (b) Zhang, S.; Painter, P. C.; Runt, J. *Macromolecules* **2002**, *35*, 8478. (c) Glema, A. J.; Mardis, K. L.; Chaudhry, A. A.; Gilson, M. K.; Payne, G. F. *Ind. Eng. Chem. Res.* **2000**, *39*, 463. (d) Wagner, K.; Schulz, S. *J. Chem. Eng. Data* **2001**, *46*, 322.
(10) (a) Wojciechowski, G.; Schroeder, G.; Zundel, G.; Brzezinki, B. *J. Phys. Chem. A* **2000**, *104*, 7469. (b) Keil, T.; Brzezinski, B.; Zundel, G. *J. Phys. Chem. A* **1992**, *96*, 4421. (c) Brzezinski, B.; Brycki, B. *J. Phys. Chem.* **1991**, *95*, 8598. (d) Nachtigall, F. F.; Lazzarotto, M.; Nome, F. J. *Braz. Chem. Soc.* **2002**, *13*, 295. (e) Ito, K.; Miki, H.; Ohba, Y. *Yakugaku Zasshi* **2002**, *122*, 413. (f) Iwasaki, A.; Fujii, A.; Watanabe, T.; Ebata, T.; Mikami, N. *J. Phys. Chem.* **1996**, *100*, 16053. (g) Felix, N.; Huyskens, P. L. *J. Phys. Chem.* **1975**, *79*, 2316. (e) Barry, J. E.; Finkelstein, M.; Ross, S. D. *J. Org. Chem.* **1984**, *49*, 1669.
(11) (a) Fang, Y.; Liu, L.; Feng, Y.; Li, X.-S.; Guo, Q.-X. *J. Phys. Chem. A* **2002**, *106*, 4669. (b) Feng, Y.; Liu, L.; Fang, Y.; Guo, Q.-X. *J. Phys. Chem. A* **2002**, *106*, 11518. (c) Foti, M. C.; Johnson, E. R.; Vinqvist, M. R.; Wright, J. S.; Barclay, L. R.; Ingold, K. U. *J. Org. Chem.* **2002**, *67*, 5190. (d) Licarini, M.; Mugnaini, V.; Pedulli, G. F.; Guerra, M. *J. Am. Chem Soc.* **2003**, *125*, 8318.
(12) (a) Zhu, W.-L.; Tan, X.-J.; Puah, C. M.; Gu., J.-D. *J. Phys. Chem. A* **2000**, *104*, 9573. (b) Makowska, J.; Makowski, M.; Gieldon, A.; Liwo, A.; Chmurzynski, L. *J. Phys. Chem. B* **2004**, *108*, 12222. (c) Abkowicz-Bienko, A. J.; Latajka, Z. *J. Phys. Chem. A* **2000**, *104*, 1004.
(13) (a) Riedl, K. M.; Hagerman, A. E. *J. Agric. Food. Chem.* **2001**, *49*, 4917. (b) Arts, M.; Haenen, G.; Wilms, L.; Beetstra, S.; Heijnen, C.; Voss, H.; Bast, A. *J. Agric. Food. Chem.* **2002**, *50*, 1184. (c) Aruoma, O. I.; Murcia, A.; Butler, J.; Halliwell, B. *J. Agric. Food. Chem.* **1993**, *41*, 1880. (d) Baratto, M. C.; Tattini, M.; Galardi, C.; Pinelli, P.; Romani, A.; Visioli, F.; Basosi, R.; Pogni, R. *Free Radiat. Res.* **2003**, *37*, 405. (e) Dufour, C.; da Silva, E.; Potier, P.; Queneau, Y.; Dangles, O. *J. Agric. Food. Chem.* **2002**, *50*, 3425.
(14) Kim, H. J.; Woo, E.; Shin, C.; Park, H. *J. Nat. Prod.* **1998**, *61*, 145. (b) Conrad, J.; Vogler, B.; Reeb, S.; Klaiber, I.; Papajewski, S.; Roos, G.; Vasquez, E.; Setzer, M. C.; Kraus, W. *J. Nat. Prod.* **2001**, *64*, 294. (c) Abram, V.; Donko, M. *J. Agric. Food Chem.* **1999**, *4*, 485. (d) Sokmen, M.; Serkedjieva, J.; Daferera, D.; Gulluce, M. *J. Agric. Food Chem.* **2004**, *52*, 3309.
(15) *Protein Architecture: Interfacing Molecular Assembly and Immobilization Biotechnology;* Lvov, Y., Mohwald, H. M., Eds.; Dekker Publ: New York, 2000; pp 1−396.
(16) (a) Wang, M.; Simon, J. E.; Aviles, I. F.; He, K.; Zheng, Q.-Y.; Tadmor, Y. *J. Agric. Food Chem.* **2003**, *51*, 601. (b) Nakamura, Y.; Tsuji, S.; Tonogai, Y. *J. Agric. Food Chem.* **2003**, *51*, 331. (c) Ikawa, M.; Schaper, T. D.; Dollard, C. A.; Sasner, J. J. *J. Agric. Food Chem.* **2003**, *51*, 1811.
(17) Antipov, A. A.; Shchukin, D.; Fedutik, Y.; Petrov, A. I.; Sukhorukov, G. B.; Mohwald, H. *Colloids Surf. A* **2003**, *224*, 175.
(18) (a) Hue, N. V.; Vega, S.; Silva, J. A. *Soil Sci Soc. Am. J.* **2001**, *65*, 153. (b) Friedman, M.; Jurgens, H. S. *J. Agric. Food. Chem.* **2000**, *48*, 2101. (c) Goldschmid, O. *Anal. Chem.* **1954**, *26*, 1421. (d) Maranville, L. F.; Goldschmid, O. *Anal. Chem.* **1954**, *26*, 1423.
(19) (a) Abbaspour, A.; Kamyabi, M. A.; Khalafi-Nezhad, A.; Soltani Rad, M. N. *J. Chem. Eng. Data* **2003**, *48*, 911. (b) Dyson, R. M.; Kaderli, S.; Lawrence, G. A.; Maeder, M.; Zuberbuhler, A. D. *Anal. Chim. Acta* **1997**, *353*, 381.
(20) Kreller, D. I.; Gibson, G.; Novak, W.; Van Loon, G. W.; Horton, J. H. *Colloids Surf. A.: Physicochem. Eng. Aspects* **2003**, *212*, 249.
(21) Flanagin, L. W.; McAdams, C. L.; Hinsberg, W. D.; Sanchez, I. C.; Willson, C. G. *Macromolecules* **1999**, *32*, 5337. Tsiartas, P. C.; Flanagin, L. W.; Henderson, C. L.; Hinsberg, W. D.; Sanchez, I. C.; Bonnecaze, R. T.; Willson, C. G. *Macromolecules* **1997**, *30*, 4656.
(22) (a) Xie, A. F.; Granik, S. *Macromolecules* **2002**, *35*, 1805. (b) Kharlampieva, E.; Sukhishvili, S. A. *Langmuir* **2003**, *19*, 1235.
(23) (a) Choi, J.; Rubner, M. F. *Macromolecules* **2005**, *38*, 116. (b) Petrov, A. I.; Antipov, A. A.; Sukhorukov, G. B. *Macromolecules* **2003**, *36*, 10079. (c) Rmaile, H. H.; Schlenoff, J. B. *Langmuir* **2002**, *18*, 8263. (d) Sui, Z.; Schlenoff, J. B. *Langmuir* **2004**, *20*, 6026. (e) Kabanov, V. *Polym. Sci.* **1994**, *36*, 143.
(24) (a) Antipov, A.; Sukhorukov, G.; Leporatti, S.; Radchenko, I.; Donath, E.; Möhwald, H. *Colloids Surf. A* **2002**, *198−200*, 535. (b) Sukhorukov, G.; Antipov, A.; Voigt, A.; Donath, E.; Mohwald, H. *Macromol. Rapid Commun.* **2001**, *22*, 44.

MA047629X